Are there stable long-range ordered $Fe_{1-x}Cr_x$ compounds?

Paul Erhart,[a] Babak Sadigh, and Alfredo Caro
Lawrence Livermore National Laboratory, Chemistry, Materials and Life Sciences Directorate, Livermore, California 94550, USA

(Received 8 November 2007; accepted 13 March 2008; published online 7 April 2008)

The heat of formation of Fe–Cr alloys undergoes an anomalous change of sign at small Cr concentrations. This observation raises the question as to whether there are intermetallic phases present in this composition range. Here, we report the discovery of several long-range ordered structures that represent ground state phases at 0 K. In particular, we have identified a structure at 3.7% Cr with an embedding energy which is 49 meV/Cr atom below the solid solution. This implies that there is an effective long-range attractive interaction between Cr atoms. We propose that the structures found in this study complete the low temperature–low Cr region of the phase diagram. © *2008 American Institute of Physics*. [DOI: 10.1063/1.2907337]

Ferritic iron-chromium alloys are important materials for structural components in fusion and fission reactors. The need to understand their behavior under irradiation has recently motivated a significant amount of basic research, the results of which have changed our understanding of these systems.[1–4] One of the most surprising and challenging observations is the coexistence of short-range order and phase segregation in the same alloy. At low Cr concentrations, both experiment[5–7] and simulations[8,9] have found a short-range ordering tendency: Cr atoms seek to maximize the number of their Fe neighbors. At larger Cr concentrations, however, phase segregation is observed, i.e., Cr atoms favor Cr neighbors. Some insight into the origin of this peculiar behavior has been provided by several first-principles calculations[1–4] which found a negative heat of formation at low Cr concentrations and an inversion of the heat of formation above approximately 10% Cr. These observations raise two important questions: (i) Are there intermetallic phases in the Fe–Cr system which are missing in the phase diagram as we know it, i.e., is there a long-range order? (ii) Is the Cr–Cr interaction in the Fe host crystal purely repulsive, i.e., do Cr atoms in Fe behave like a lattice gas, or is there an effective attraction between the Cr atoms? In the following, we will demonstrate by means of density-functional theory (DFT) calculations that (i) there are several intermetallic phases at small Cr concentrations and that (ii) some of these phases correspond to an effective *long-range attractive* interaction between the Cr atoms.

In order to motivate our approach, we show in Fig. 1 a schematic plot which illustrates the consequences of both purely repulsive as well as attractive effective interactions between the Cr atoms. For the following qualitative discussion, we treat the Fe matrix as an effective medium into which the Cr atoms are embedded. The energy gained if a single Cr atom is removed from a bulk Cr crystal and inserted into a pure Fe matrix defines the heat of solution for a single (isolated) impurity, i.e., the *embedding energy* at infinite dilution, which is indicated by the horizontal dashed lines in Figs. 1 and 2(a). In the case of purely repulsive Cr–Cr interactions, adding any other number of Cr atoms can only render the embedding energy *per Cr atom* less negative, which leads to the shaded region in Fig. 1. In contrast, if attractive forces are present, there will be configurations in which the embedding energy per Cr atom is *more* negative than the dilute limit, as indicated by the solid circles in Fig.

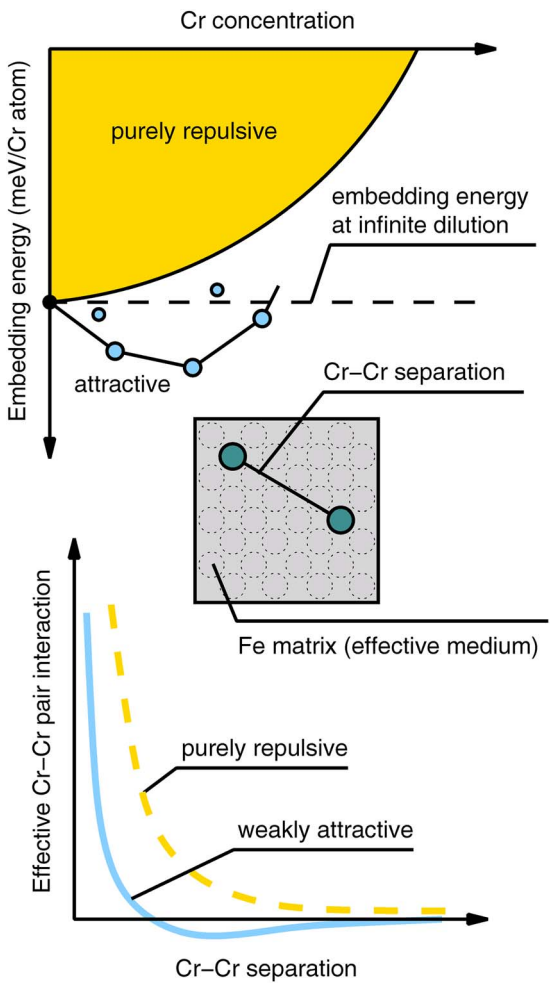

FIG. 1. (Color online) Purely repulsive vs weakly attractive interactions. If the Cr–Cr interaction is purely repulsive, the embedding energy per Cr atom for any possible configuration can only be less negative than the embedding energy at infinite dilution. If there is, however, some effective attraction between the Cr atoms, intermetallic phases exist and there are structures for which the embedding energy per Cr atom lies below the infinite dilution limit.

[a]Electronic mail: erhart1@llnl.gov.

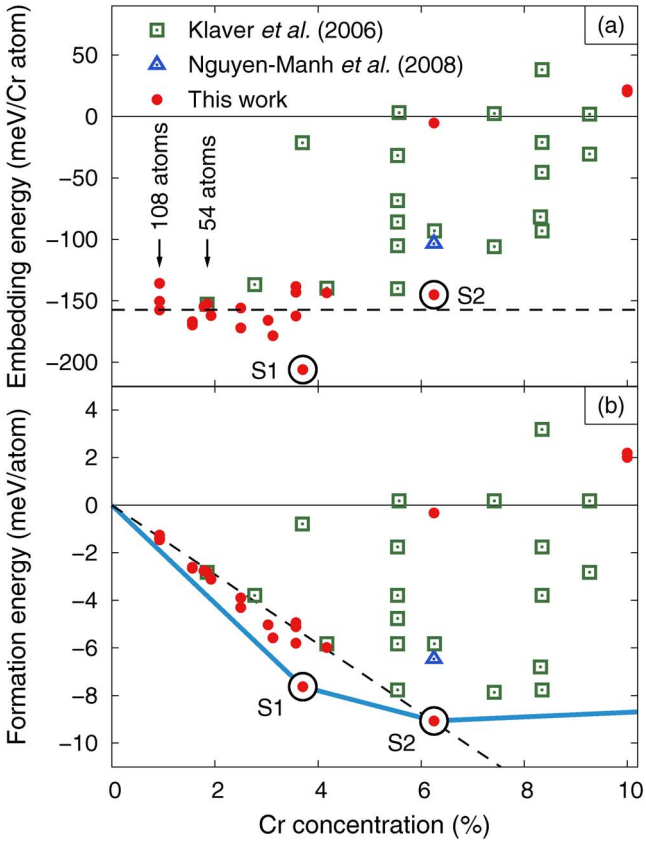

FIG. 2. (Color online) Calculated formation energies plotted (a) as embedding energy per Cr atom and (b) formation energy per atom. In (a), the structure with the lowest formation energy per Cr atom is marked by S1. In this structure the Cr atoms occupy a bcc sublattice three times as large as the underlying Fe bcc lattice. In (b), the most stable intermetallic phases, S1 and S2 are connected by thick solid lines. For compositions which fall on these lines, the system decomposes into a two-phase mixture. For concentrations above 6.25% Cr, the thick solid line connects S2 with pure Cr.

2. In either case, since the alloy segregates for larger amounts of Cr, the embedding energy must eventually become positive as more and more Cr atoms are added. Finally, it should be noted that in the case of purely repulsive interactions, intermetallic phases are possible but need not exist. However, if the interaction is attractive, intermetallic phases *must* exist.

In alloy thermodynamics, instead of considering the embedding energy, it is more common to describe a system in terms of the formation energy (identical to the mixing energy in the case of a random system), which is the energy *per atom* of the alloy compared to the fully separated components (both Fe and Cr). If one adopts this view, the embedding energy at infinite dilution determines the slope of the dashed line in Fig. 2(b). If the Cr–Cr interaction is purely repulsive, all configurations with finite Cr concentration lie *above* this line, whereas at least some phases must lie *below* this line if there is some attraction.

In several previous studies,[4,8,10,11] the formation energies of a number of Fe–Cr configurations were calculated by using the supercells derived from the conventional two-atom body-centered-cubic (bcc) cell (also compare Fig. 1). On the basis of these data, one would have to conclude that the interaction between Cr atoms is purely repulsive.

In the present study, we have followed an alternative approach. We systematically generated a large number of structures in which the Cr atoms selectively occupy certain neighbor shells. No restrictions were imposed with regard to the symmetry of the Cr sublattice. Specifically, we did not construct our supercells on the basis of the conventional two-atom bcc unit cell but considered multiples of the primitive cell. Any supercell employed in the present work contains exactly one Cr atom and is uniquely determined by an integer matrix $\boldsymbol{A}$, which relates the matrix of primitive cell vectors $\boldsymbol{h}$ to the vectors spanning the supercell $\boldsymbol{H}$,

$$\boldsymbol{H} = \boldsymbol{A}\boldsymbol{h}, \quad \boldsymbol{h} = \frac{1}{2}\begin{pmatrix} -1 & 1 & 1 \\ 1 & -1 & 1 \\ 1 & 1 & -1 \end{pmatrix}, \tag{1}$$

Note that the determinant of $\boldsymbol{A}$ equals the number of atoms in the supercell. By using the appropriate matrices $\boldsymbol{A}$, one can construct supercells with a variety of different symmetries. Specifically, supercells with face-centered-cubic (fcc) and simple cubic (sc) symmetries are obtained if one uses integer multiples of the matrices

$$\boldsymbol{A}_{\mathrm{fcc}} = \begin{pmatrix} 2 & 1 & 1 \\ 1 & 2 & 1 \\ 1 & 1 & 2 \end{pmatrix}, \quad \boldsymbol{A}_{\mathrm{sc}} = \begin{pmatrix} 0 & 1 & 1 \\ 1 & 0 & 1 \\ 1 & 1 & 0 \end{pmatrix}. \tag{2}$$

We generated a large set of different supercells focusing on the structures with a depletion of Cr atoms in the first five neighbor shells. We then employed DFT to calculate the total energies for these structures[19] and obtained the formation energies from

$$\Delta E = E_{\mathrm{FeCr}} - n_{\mathrm{Fe}}/(n_{\mathrm{Fe}} + 1)E_{\mathrm{Fe}} - E_{\mathrm{Cr}}, \tag{3}$$

where n_{Fe} denotes the number of Fe atoms in the supercell, E_{FeCr} is the total energy for the supercell, E_{Fe} is the total energy of the structurally identical pure Fe cell, and E_{Cr} is the energy per atom obtained from a primitive antiferromagnetic Cr cell. If ΔE is divided by the number of Cr atoms in the cell, one obtains the embedding energy per Cr atom ΔE_{emb}, whereas division by the total number of atoms yields the formation energy ΔE_f. Special care was taken to minimize the error in our calculations by varying the cell shape and volume to reduce the strain effects. Formation energies were exclusively calculated as differences between fully equivalent supercells by using fully equivalent k-point grids.

The key results of our calculations are compiled in Fig. 2. The embedding energy at infinite dilution has been obtained using a 108-atom fcc supercell (0.9% Cr). For this structure, the neighbor shells of any Cr atom are depleted of other Cr atoms except for the 25th shell for which 12 out of 36 neighbors are Cr. This corresponds to a Cr–Cr separation of $4.24a_0$ along the $\langle 411 \rangle$ direction where a_0 is the bcc lattice parameter. The embedding energy obtained for this cell is −157 meV/Cr atom, and henceforth is considered as the infinite dilution limit. For comparison, the lowest concentration of 1.9% considered in previous studies corresponds to a structure in which the closest Cr–Cr separation is $3a_0$ along the $\langle 300 \rangle$ direction and which yields an embedding energy of −153 meV/Cr atom.

Our most important discovery is that there are several structures, the energies of which lie below the line given by the infinite dilution limit. According to the above discussion, the location of these data points implies that there is a net attractive interaction between Cr atoms. The structure which shows by far the lowest energy per Cr atom is marked in Fig. 2 by the leftmost black circle (S1). In this 27-atom supercell

with 3.7% Cr, the Cr atoms are arranged on a bcc superlattice three times as large as the underlying bcc Fe lattice. The first nine neighbor shells are exclusively occupied by Fe atoms, whereas the tenth shell is filled to one quarter by Cr atoms. The Cr–Cr pairs are aligned along the ⟨111⟩ direction and separated by $2.60a_0$. The embedding energy for this structure is −206 meV/Cr atom, which is 49 meV/Cr atom below the infinite dilution limit. There are several other structures at concentrations smaller than 3.7% Cr with energies below the infinite dilution limit. They resemble the lowest energy structure in that they display a depletion of Cr atoms at short range and partly or fully Cr filled shells at longer range.

For concentrations larger than 3.7% Cr, the structure with the lowest energy (S2 in Fig. 2) is based on a 16-atom base-centered monoclinic unit cell with lattice vectors

$$\boldsymbol{H} = \frac{1}{2}\begin{pmatrix} -1 & 3 & 3 \\ 3 & -1 & 3 \\ 3 & 3 & 1 \end{pmatrix}, \quad \boldsymbol{A} = \begin{pmatrix} 3 & 1 & 1 \\ 1 & 3 & 1 \\ 2 & 2 & 3 \end{pmatrix}. \tag{4}$$

The S2 structure has an embedding energy of −145 meV/Cr atom equivalent to a formation energy of −9.1 meV/atom. In order to describe this structure on the basis of the conventional two-atom unit cell, one would have to employ a $16\times16\times8$ (4096 atom) supercell. The S2 structure described here is different from the intermetallic structure described in Refs. 10 and 11, although both structures correspond to a Cr concentration of 6.25%. The structure described in Refs. 10 and 11, however, can be represented in a $2\times2\times2$ (16 atom) cubic supercell in which the Cr atoms are arranged on a simple cubic lattice with a lattice constant which is twice as large as the lattice constant of the underlying bcc Fe matrix. Furthermore, its formation energy is only −6.5 meV/atom (compare the open triangle in Fig. 2 and Ref. 11), and thus is not as negative as the value of −9 meV/atom calculated for the S2 structure.

In order to determine the zero temperature phase diagram, we consider the energy per total number of atoms (formation energy), as shown in Fig. 2(b). The infinite dilution limit is indicated by the dashed line and the stable phases are connected by thick solid lines, along which the system decomposes into two-phase mixtures. The two relevant intermetallic ground state phases occur at 3.7% (S1) and 6.25% (S2) corresponding to the two structures described above.

It is important to address the magnitude of the observed effect. Even for the most optimal structures, the energy gain per atom amounts to merely 10 meV/atom, which corresponds to approximately 110 K. At higher temperatures, the configurational entropy favors the solid solution. Due to the reduced atomic mobility at these low temperatures direct experimental observation of the ordering may be challenging. Nevertheless, our discovery suggests that the low temperature phase diagram of Fe–Cr alloys is more complex than previously thought.

In summary, in this letter, we have demonstrated that there are intermetallic ground state phases at the Fe-rich end of the Fe–Cr phase diagram with embedding energies as low as −206 meV/Cr atom and formation energies as low as −9 meV/atom. The observation of embedding energies below the infinite dilution limit implies that there are effective long-range attractive interactions between the Cr atoms which are the result of many-body effects. In fact, attempts to capture the observed behavior in terms of simple pair interaction models were unsuccessful. Extensive further study is required to elucidate the physical origin of this phenomenon.

This work performed under the auspices of the U.S. Department of Energy by Lawrence Livermore National Laboratory under Contract No. DE-AC52-07NA27344 with support from the Laboratory Directed Research and Development Program. Generous grants of computer time through the National Energy Research Scientific Computing Center at Lawrence Berkeley National Laboratory are gratefully acknowledged.

[1] M. Hennion, J. Phys. F: Met. Phys. **13**, 2351 (1983).
[2] A. A. Mirzoev, M. M. Yalalov, and D. A. Mirzaev, Phys. Met. Metallogr. **97**, 336 (2004).
[3] P. Olsson, I. A. Abrikosov, and J. Wallenius, Phys. Rev. B **73**, 104416 (2006).
[4] T. P. C. Klaver, R. Drautz, and M. W. Finnis, Phys. Rev. B **74**, 094435 (2006).
[5] V. V. Ovchinnikov, N. V. Zvigintsev, V. S. Litvinov, and V. A. Osminkin, Fiz. Met. Metalloved. **42**, 310 (1976).
[6] I. Mirebeau, M. Hennion, and G. Parette, Phys. Rev. Lett. **53**, 687 (1984).
[7] V. V. Ovchinnikov, B. Y. Goloborodsky, N. V. Gushchina, V. A. Semionkin, and E. Wieser, Appl. Phys. A: Mater. Sci. Process. **83**, 83 (2006).
[8] M. Y. Lavrentiev, R. Drautz, D. Nguyen-Manh, T. P. C. Klaver, and S. L. Dudarev, Phys. Rev. B **75**, 014208 (2007).
[9] P. Erhart, A. Caro, M. S. de Caro, and B. Sadigh, "Short-range order and precipitation in Fe-rich Fe–Cr alloys," Phys. Rev. B (in press).
[10] D. Nguyen-Manh, M. Y. Lavrentiev, and S. L. Dudarev, C. R. Phys. (unpublished).
[11] D. Nguyen-Manh, M. Y. Lavrentiev, and S. L. Dudarev, Scientific Modeling and Simulation **14**, 159 (2007).
[12] G. Kresse and J. Hafner, Phys. Rev. B **47**, 558 (1993).
[13] G. Kresse and J. Hafner, Phys. Rev. B **49**, 14251 (1994).
[14] G. Kresse and J. Furthmüller, Phys. Rev. B **54**, 11169 (1996).
[15] G. Kresse and J. Furthmüller, Comput. Mater. Sci. **6**, 15 (1996).
[16] P. E. Blöchl, Phys. Rev. B **50**, 17953 (1994).
[17] G. Kresse and D. Joubert, Phys. Rev. B **59**, 1758 (1999).
[18] J. P. Perdew, K. Burke, and M. Ernzerhof, Phys. Rev. Lett. **77**, 3865 (1996); **78**, 1396(E) (1997).
[19] Calculations were carried out within density-functional theory using VASP (Refs. 12–15) with the projector augmented plane-wave method (Refs. 16 and 17). The spin-polarized generalized gradient approximation in the parametrization by Perdew, Burke, and Ernzerhof was employed to represent the exchange-correlation potential (Ref. 18). The *k*-point grids for Brillouin zone integrations were chosen to ensure a total energy convergence of at least 1 meV/Cr atom. For Fe, the 4*s* and 3*d* electrons were included in the valence, and the Cr pseudopotential included the 4*s*, 3*d*, and 3*p* electrons.